ARL-TR-7741 ● AUG 2016

US Army Research Laboratory

Blast-Loading Assessment of Multi-Energy Flash Computed Tomography (MEFCT) Diagnostic

by Michael B Zellner, Charles L Randow, Ronald Cantrell, and Corey E Yonce

NOTICES

Disclaimers

The findings in this report are not to be construed as an official Department of the Army position unless so designated by other authorized documents.

Citation of manufacturer's or trade names does not constitute an official endorsement or approval of the use thereof.

Destroy this report when it is no longer needed. Do not return it to the originator.

ARL-TR-7741 ● AUG 2016

US Army Research Laboratory

Blast-Loading Assessment of Multi-Energy Flash Computed Tomography (MEFCT) Diagnostic

Michael B Zellner, Charles L Randow, Ronald Cantrell, and Corey E Yonce
Weapons and Materials Research Directorate, ARL

REPORT DOCUMENTATION PAGE

Form Approved
OMB No. 0704-0188

1. REPORT DATE *(DD-MM-YYYY)*	2. REPORT TYPE	3. DATES COVERED (From - To)
August 2016	Technical Report–Final	October 2015–September 2016

4. TITLE AND SUBTITLE
Blast Loading Assessment of Multi-Energy Flash Computed Tomography (MEFCT) Diagnostic

5a. CONTRACT NUMBER

5b. GRANT NUMBER

5c. PROGRAM ELEMENT NUMBER

6. AUTHOR(S)
Michael B Zellner, Charles L Randow, Ronald Cantrell, and Corey E Yonce

5d. PROJECT NUMBER
AH80

5e. TASK NUMBER

5f. WORK UNIT NUMBER

7. PERFORMING ORGANIZATION NAME(S) AND ADDRESS(ES)
US Army Research Laboratory
ATTN: RDRL-WMP-D
Aberdeen Proving Ground, MD 21005-5069

8. PERFORMING ORGANIZATION REPORT NUMBER
ARL-TR-7741

9. SPONSORING/MONITORING AGENCY NAME(S) AND ADDRESS(ES)

10. SPONSOR/MONITOR'S ACRONYM(S)

11. SPONSOR/MONITOR'S REPORT NUMBER(S)

12. DISTRIBUTION/AVAILABILITY STATEMENT
Approved for public release; distribution is unlimited.

13. SUPPLEMENTARY NOTES

14. ABSTRACT
The US Army Research Laboratory is developing a Multi-Energy Flash Computed Tomography (MEFCT) diagnostic that will be used to capture tomographic image(s) of dynamic events. To accomplish dynamic tomography, the diagnostic uses numerous source–detector pairs to accumulate fifteen 2-D images, which are subsequently used for reconstruction of up to three 3-D tomograms spaced in time. This work assesses the robustness of the support structure that houses the 15 source–detector pairs, quantifies real-time measurements of source and detector movement during blast loading, and addresses the implications of these movements on the reconstruction process.

15. SUBJECT TERMS
blast, pressure gauge, flyer plate, overpressure, computed tomography, photon Doppler velocimetry, accelerometer

16. SECURITY CLASSIFICATION OF:			17. LIMITATION OF ABSTRACT	18. NUMBER OF PAGES	19a. NAME OF RESPONSIBLE PERSON
a. REPORT	b. ABSTRACT	c. THIS PAGE			Michael B Zellner
Unclassified	Unclassified	Unclassified	UU	26	19b. TELEPHONE NUMBER (Include area code) 410-278-1183

Contents

List of Figures

List of Tables

Acknowledgments

The authors would like to acknowledge enlightening conversations with R Becker and K Uhlig of the US Army Research Laboratory (ARL) Weapons and Materials Research Directorate's Impact Physics Branch concerning development and testing of the structure. They would also like to thank K Dudeck and C Benjamin of the ARL Weapons and Materials Research Directorate's Multi-Threat Armor Branch as well as the ARL weld-shop and Range 7a personnel for their support in construction of the Multi-Energy Flash Computed Tomography diagnostic and testing.

1. Introduction

The US Army Research Laboratory (ARL) is developing an X-ray-based Multi-Energy Flash Computed Tomography (MEFCT) diagnostic that will be used to capture tomographic image(s) of dynamic events. The diagnostic will be used to quantitatively assess material response during experiments including ballistic impact of targets, high-explosive acceleration of materials, and high-speed mixing of fragmented materials. This system will provide advantages over conventional flash radiography in that it will have the capability to make observations in the form of 3-frame, 3-D density radiogram movies or a single 3-D density snapshot that includes definition of up to 3 materials plus void (i.e., it will be capable of differentiating between compressed acrylic and noncompressed glass when they have similar densities).

Conception of this diagnostic derived from observations of conventional and energy-selective medical X-ray computed tomography,[1] high-speed computed tomography,[2] numerous advances in iterative computed-tomography reconstruction methods,[3,4] and advances in computational capabilities (both central processing unit and graphics processing unit).[5,6] Because this diagnostic will be computing a tomogram, all criteria derived from conventional methods still apply: adequate signal-to-noise, precise knowledge of the source–detector pair's location, complete understanding of the X-ray photon spectrum, knowledge of Compton scattered X-ray photons, and so on. However, dynamic tomography of the desired events dictates that the timescale of acquisition be reduced to the order of 100 ns to prevent motion blur. The system may also be subject to potential nuisance impulsive-loading interactions from the dynamic targets/materials.

To perform dynamic tomography, ARL constructed a set of 3 concentric aluminum rings that will support five 150-keV source–detector pairs, five 300-keV source–detector pairs, and five 450-keV source–detector pairs. All of the detector pairs are oriented to image an object at the ring center (see Fig. 1). The system will use L-3 Communication's flash X-ray sources[7] paired with Carestream Dental's digital imaging plates[8] to acquire 2-D radiographs of the target from varying angular perspectives. The different angular perspectives will be used for the recombination process.[2,9] This method addresses the temporal issues associated with dynamic tomography, as the L-3 systems produce an X-ray pulse for a duration of approximately 60–80 ns. However, this method complicates the computation of the 3-D tomogram because of individualistic photon-intensity spectrums and may influence the ability to accurately know the sources' or detectors' positions at the time of acquisition when subject to loading impulses.

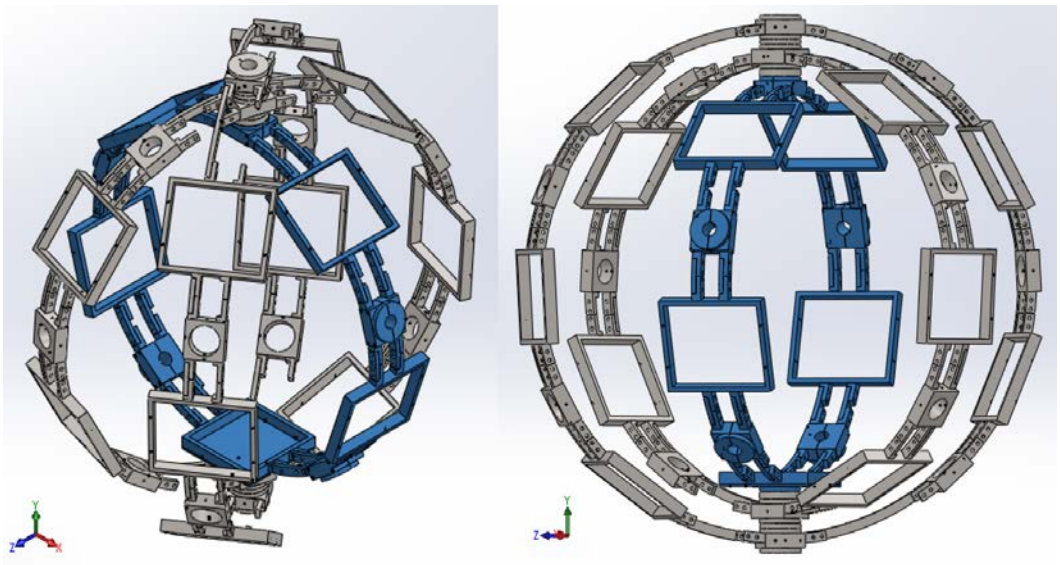

Fig. 1 Schematic depiction of the MEFCT's support structure; interior ring is in blue

This work assesses the robustness of the support structure that houses the 15 source–detector pairs, makes in situ measurements of source and detector movement during blast loading, and addresses the implications of these movements on the reconstruction process. (The implications of individualistic X-ray flux spectra will be addressed at a later time.) High-speed photography, photon Doppler velocimetry (PDV), and multiaxis accelerometers were used to accurately measure the structure's global movement during high-explosive-generated blast-impulsive exposure. Measurements were made during incremental loadings of 91–545 g of military-grade Detasheet C sheet explosive—63% pentaerythritol tetranitrate (better known as PETN), 8% nitrocellulose binder, 29% acetyl tributyl citrate (also known as ATBC)—which equates to 0.25–1.5 lb of TNT equivalent.[10]

2. Experimental Setup

To assess the robustness and real-time movement of the MEFCT system, we subjected the interior support ring (colored blue in Fig. 1) to blast created by detonation of Detasheet C high explosive. In all cases, the high explosive was supported at the center of the ring structure (ring radius ~ 1 m) using a protruding 25- × 100- × 600-mm closed-cell, polyethylene-foam arm secured to a wooden stand. The high explosive was made from a stack of sheet explosive with the largest-area sheets on the bottom (as defined by gravity). The stack was initiated using an RP-80 explosive bridge-wire detonator[11] affixed to the center of the top sheet of explosive. Figure 2 depicts the setup.

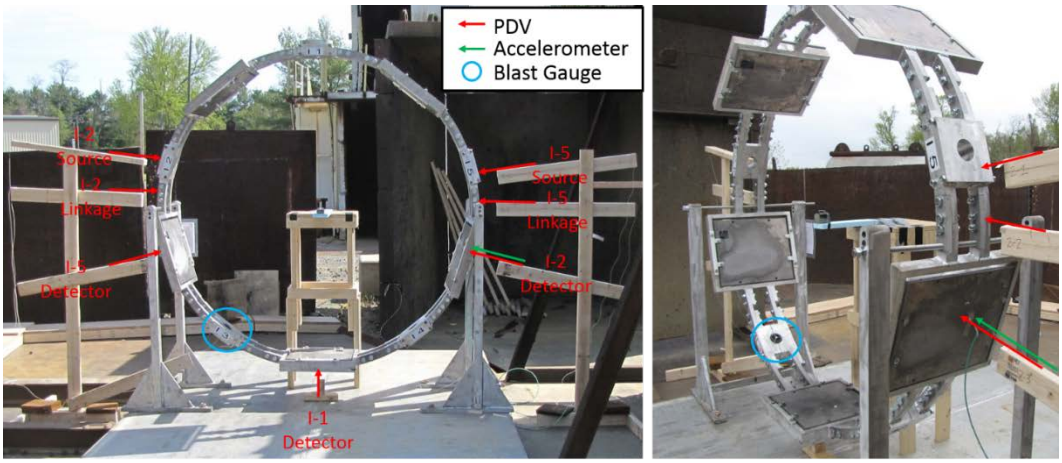

Fig. 2 Geometry used to blast load the interior ring of the MEFCT support structure: red arrows show where PDV was used to measure the displacement; green arrows show where accelerometers were used to measure the displacement; and the blue circle shows where a blast gauge was used to measure the loading exerted on the support structure

The Table summarizes the MEFCT experiments and the relevant parameters.

Table List of the high-explosive experiments with relevant parameters

Test No.	Date	Detasheet C weight (g)	Equivalent TNT weight (g, lb)	High-explosive geometry	Detonator
7a-52	4/21/16	91	115, 0.25	4 ea. 50- × 50-mm C5 sheets, 3 ea. 50- × 50-mm C1 sheets, 1 ea. 25- × 25-mm C1 sheet.	RP-80
7a-53	4/21/16	182	231, 0.5	9 ea. 50- × 50-mm C5 sheets, 1 ea. 50- × 25-mm C5.	RP-80
7a-54	4/22/16	364	463, 1.0	11 ea. 63.5- × 63.5-mm C5 sheets, 1 ea. 50- × 50-mm C5 sheet.	RP-80
7a-55	4/22/16	545	692, 1.5	13 ea. 73- × 73-mm C5 sheets, 1 ea. 73- × 71-mm C5 sheet.	RP-80

Real-time ring motions were captured via high-speed photography, PDV,[12–14] and multiaxis accelerometers at numerous points (as indicated by Fig. 2). In addition a PDV-based blast gauge[15] was used to quantify the blast pressure at a location where a 150-keV tube would be mounted.

The high-speed photography was performed with a Photron SAE 1.1 silicon-based, charge-coupled device (CCD) camera. The CCD camera was triggered upon detonation of the high explosive and captured 1,024 × 1,024 pixel images at frame rates between 5,000 and 10,000 frames per second, depending on the experiment.

Illumination was provided by ambient light. Using these spatial and temporal settings, the diagnostic was capable of discerning movement of objects in the plane of the support structure ring that translated 2.2 mm over 100 or 200 µs, respectively.

The photon Doppler velocimetry was performed at 7 individual points along the ring structure and the ejectable detector packs. Four of the points were acquired using one system denoted "PDV1", and 3 of the points were acquired using a second system denoted "PDV2". PDV1 consisted of 4 Third Millennium Engineering F177a mod-block PDV units[16] that use a 10-GHz PIN photodiode, integrated with a 2-watt IPG ELR-2-1550-LP-SF Erbium-based fiber laser[17] and a Keysight DSOX9000 oscilloscope.[18] PDV2 consisted of 4 Third Millennium Engineering F179a mod-block PDV units run in homodyne mode that use a 10-GHz PIN photodiode, integrated with a 2-watt IPG ELR-2-1550-LP-SF Erbium-based fiber laser and an Agilent DSOS600 oscilloscope. In all cases, the scopes were triggered off a Pearson inductive coil that monitored electrical impulse to the detonator and recorded data at a rate of 1 GSam/s. At each position, a single probe was used to measure the velocity with its position aligned with the plane of the ring, pointing toward the ring's center. The light-collimating probe was provided by AC Photonics[19] (PN: 1CL15A300LSD01-4m) and had a 400-mm working distance.

A single multiaxis accelerometer was used to measure the motion of an ejectable detector pack. It was firmly mounted via epoxy approximately 20 mm from the point characterized by PDV2's Probe 3 on a rigid-body ejectable detector pack. The accelerometer was an Analog Devices ADXL335, which is mounted to a complete board. It is capable of measuring accelerations of ± 3g. The outputs were coupled to ground via a 0.1-µf capacitor resulting in approximately 50 Hz of temporal resolution. The signals from the 3 outputs were recorded on an Agilent DSO6000 oscilloscope that was cotriggered with the PDV oscilloscope.

The PDV-based blast gauge was mounted so that its free-flying puck was positioned where the surface of a 150-keV X-ray tube's head would be in the MEFCT diagnostic. Friction held the gauge in place. To enhance the coupling, approximately 10 mm of neoprene rubber was wrapped around the gauge's acrylic body, which was then compressed when the aluminum tube holder was tightened. This resulted in a firm mounting in which the acrylic gauge body remained stationary—even when loading was sufficient to eject the puck and the PDV probe holder, which was tightly press-fit into the body of the gauge. Figure 3 is a photograph of the blast gauge in this mounting.

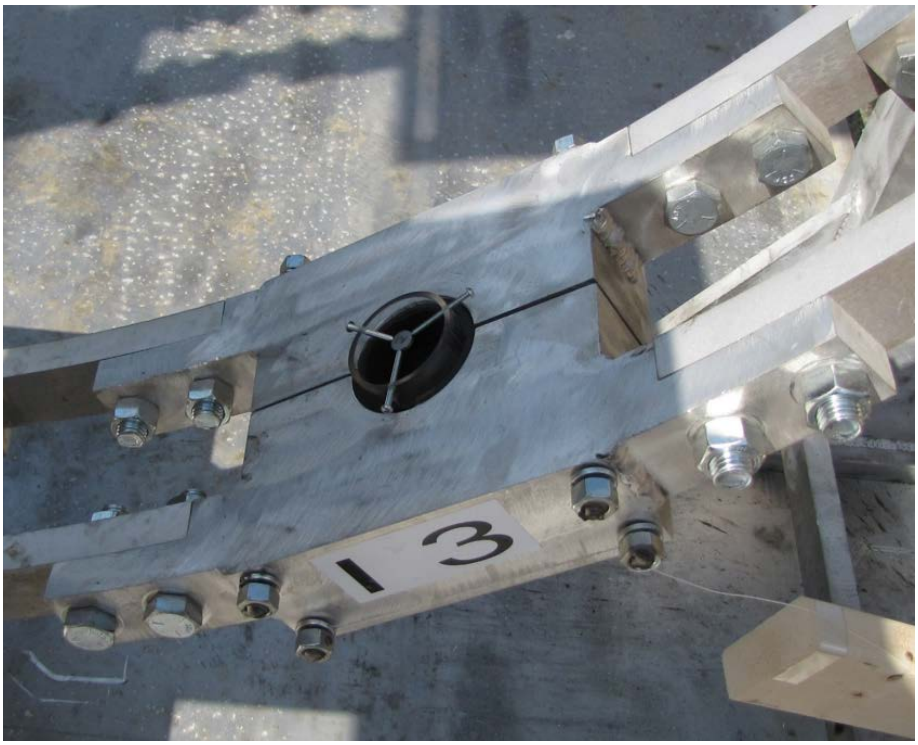

Fig. 3 Mounting of the blast gauge inside the Interior (I)-3 source location of the MEFCT support structure

3. Results and Discussion

The geometry of the high explosive prior to its detonation resulted in directional, nonspherical loading of the support structure. This directionality, which was captured using photography, propels primary compression fronts and debris clouds orthogonal to the faces of the high-explosive stack, as shown in Fig. 4. The compression front propagates more slowly in the intermediate locations (highlighted with yellow in Fig. 4). The impulse measurements were acquired on the X-ray source mounts, support structure linkages, and detector packs that were aligned with directions of primary blast during the experiment.

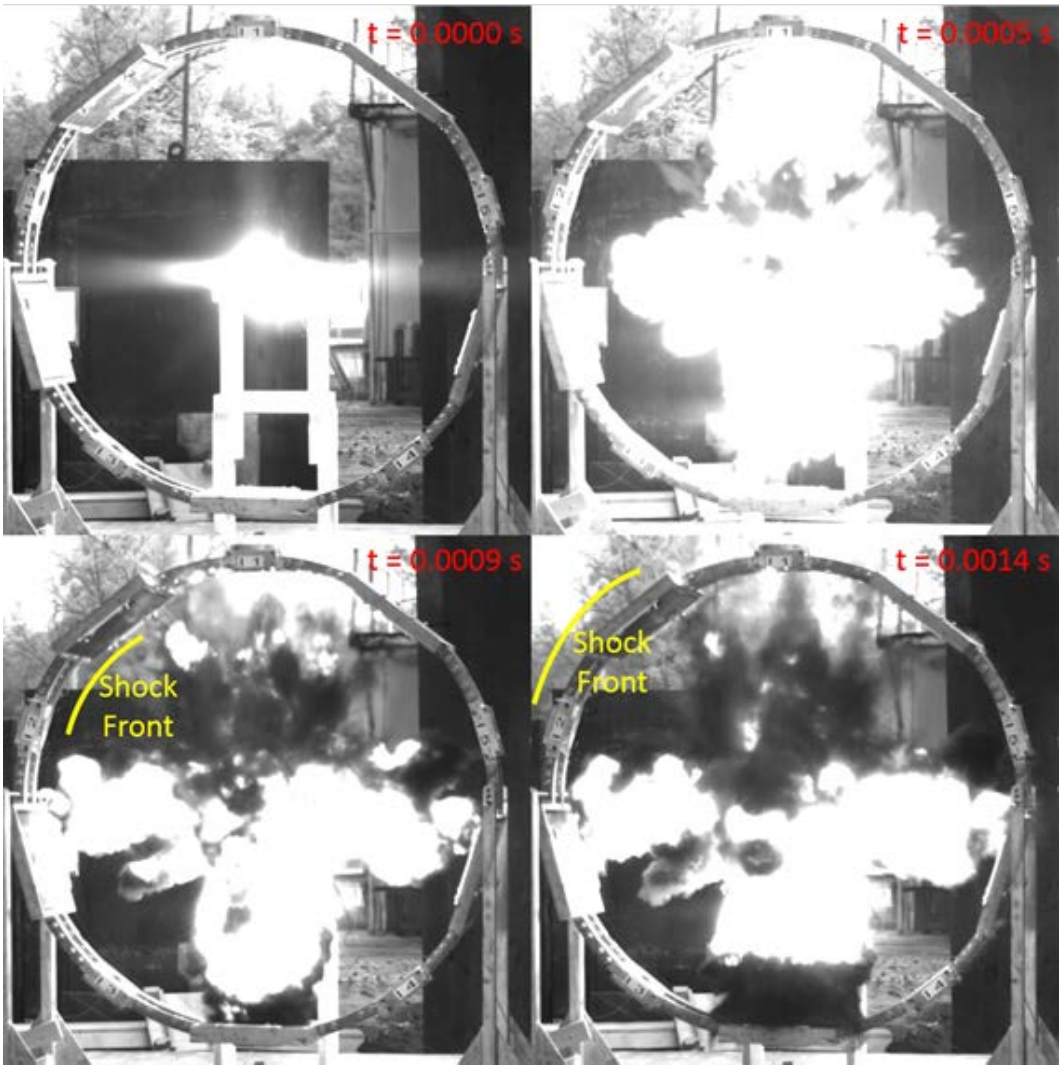

Fig. 4 Detonation geometry of Detasheet C high explosive inside the MEFCT support structure; shock front propagating within the intermediate region is highlighted in yellow in the last 2 images

Because the X-ray detector packs comprise the majority of the exposed support structure's surface area subject to blast, the MEFCT diagnostic incorporates use of nylon shear tabs to affix the packs inside the aluminum frame. The detector packs are designed to fly free upon shearing, minimizing the frame loading to that which occurs just prior to shearing. In our experiments, detonation of total high-explosive weights of up to 364 g left the plastic shear tabs along the primary directions intact (some plastically deformed). For a total high-explosive weight of 545 g, the tabs sheared resulting in complete release along the main loading direction and no shearing along the intermediate directions. Figure 5 shows images of the shear tabs

from the I-2 detector. Further analysis within this work will focus on these 2 situations, as they are assumed to be the 2 most stressful loadings placed on the support structure (one symmetric and one asymmetric).

Fig. 5 The detectors and shear tabs following experiments in which 364 g and 545 g of Detasheet C were detonated at the center of the MEFCT support structure

Figure 6 shows the PDV spectrogram generated from Doppler-shifted light that reflected off the I-2 detector's rear surface; it also has a fit to the data (black overlay). This spectrogram is typical to the type of data collected in that there is a primary reflection that first displaces and later becomes oscillatory. It is also typical to detect weaker reflections throughout, possibly originating from ejected dust and oxide layers, engulfing soot and high-explosive debris, and movement of the PDV light-collimating probe.

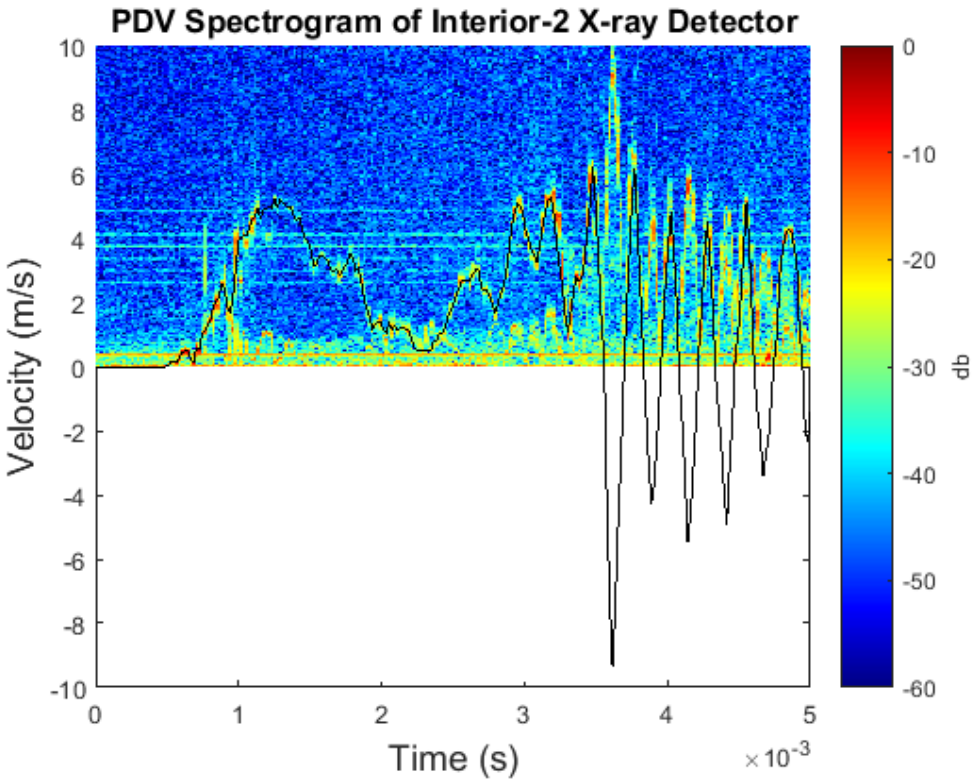

Fig. 6 Spectrogram depicts a typical result from movement of a detector after detonation of high explosive at the center of the MEFCT support structure. A fit to the spectrogram is overlaid in black.

Figure 7 shows the radial displacement versus time of 4 locations with respect to the time of detonation: the I-5 source, the I-5 (support) linkage, the I-2 detector, and the I-1 detector. At the I-5 source location, first movement was detected approximately 0.5 ms after detonation of the high-explosive charge. This value indicates an overdriven shock was generated in the air, and the velocity of the shock front will be dependent on the energy release of the high explosive. In the time spanning 0.5 ms to 4 ms, displacement of 6 mm was measured when a 364-g charge of explosive was detonated, and approximately 1 mm was measured when a 545-g charge was detonated. Differences in displacement magnitude may be attributed to the flex/slip associated with the structural bolting or elastic displacements of the ring structure when elevated asymmetries arise resultant of the packs' failure to fully eject and/or from detonation asymmetries. The displacement at the I-5 linkages of both shots demonstrate less movement than at the I-5 source locations. At this location, the movement appears similar in magnitude regardless of the high-explosive charge's size. The lesser displacement at the linkage locations are most likely attributed to the reduced surface area of the linkage exposed to the blast front. Because of the oscillatory nature of the velocity spectrograms it is also possible that incorrect inflections were selected and, therefore, resulted in an incorrect sign when

integrating the results to distance. This could increase or decrease the displacement but (in the authors' opinion) not likely more than a factor of 2, and these implications are well past the time for desired measurements.

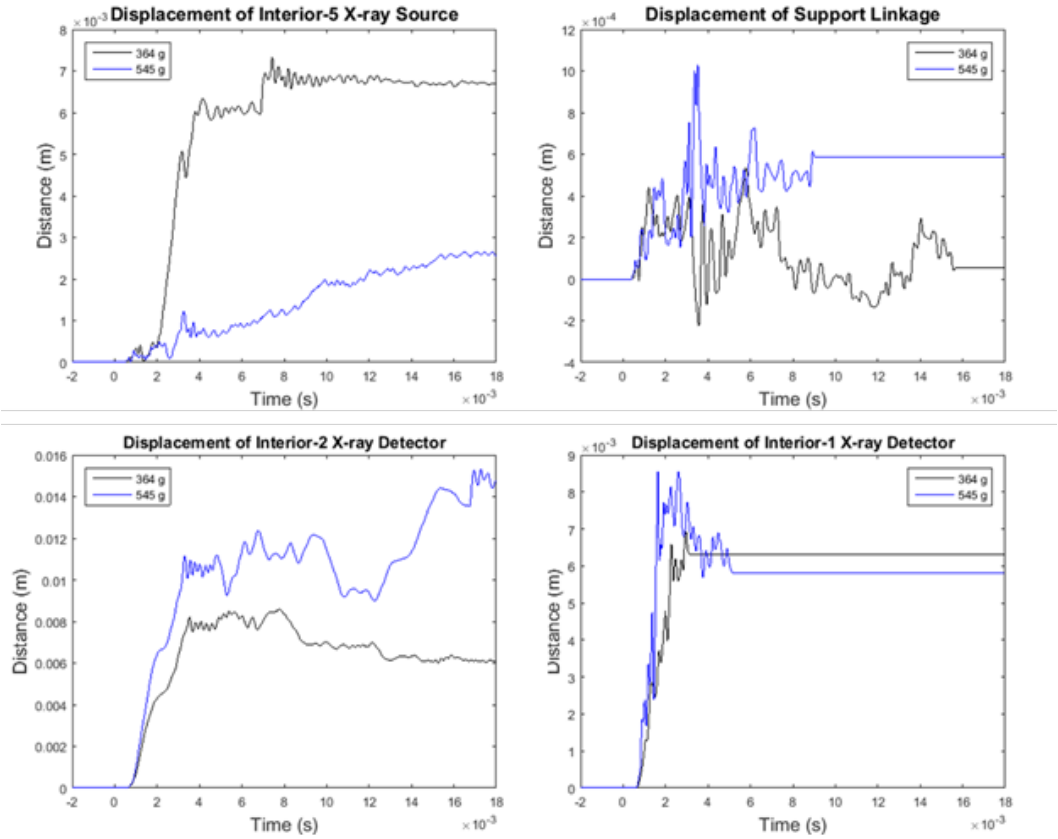

Fig. 7 Displacement measurements acquired with PDV, in situ, during acceleration from detonation of 364 g and 545 g of Detasheet C high explosive at the center of the MEFCT support structure

The displacements of the I-2 and I-1 detectors display increased rates and magnitudes as the explosive loadings are increased. The important distinction here is the detectors at location I-2 are allowed to fly free whereas the detector at location I-1 is firmly mounted to the ring, as it will be a pivot point when this interior ring is nested inside the outer 2 rings of the MEFCT diagnostic. Because the I-1 detector is firmly mounted and has a smaller surface area then the I-1 source, a symmetric drive will produce asymmetric loading on the ring structure, causing downward movement. In this setup, this asymmetric-ring-loading condition will be fully exerted on the 2 support stands; however, in the full-up MEFCT diagnostic, the solid pivot point will also be supported, resting on the 10-ft × 8-ft × 3-inch solid-aluminum support plate.

Postmortem examination indicated no plastic deformation was exerted into the MEFCT aluminum support structure or into the 3/4-inch (19-mm)-diameter Grade 5 bolts used to affix the structure, up to the 545-g Detasheet C high-explosive loading applied. This is supported by the results of the PDV blast gauge, which recorded the impulse exerted at the I-3 source position. Figure 8 shows the PDV spectrogram and the acceleration profile of the PDV blast gauge for the 545-g Detasheet C experiment. The puck used in the PDV blast gauge weighed 2.0 g. The measurements show accelerations on the order of 3.5 $*10^4$ m/s^2, which computes to an impulse peaking near 70 N and a ΔP applied to the gauge puck[20] peaking near 6 * 10^5 Pa, as shown in Fig. 9. This pressure is well below the elastic yield strength of aluminum (240 MPa) or the tensile strength of the Grade 5 bolts (830 MPa) used to affix the structure.

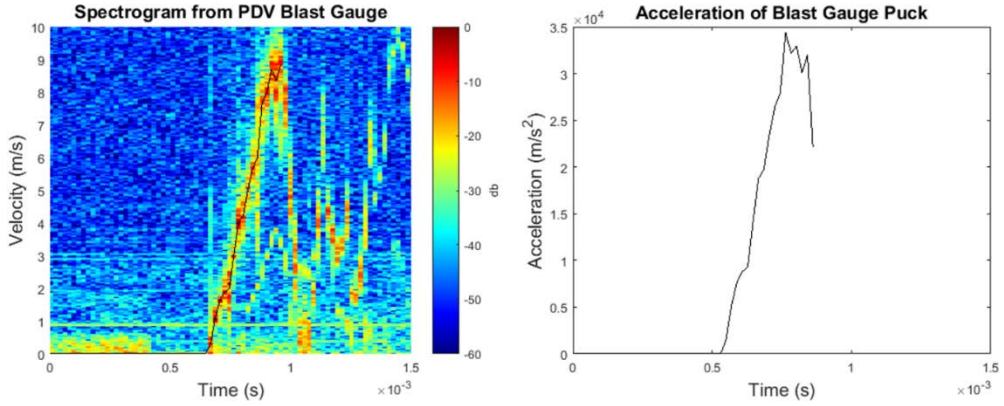

Fig. 8 PDV-measured acceleration of the disk within a blast gauge positioned at the I-3 source location of the MEFCT diagnostic

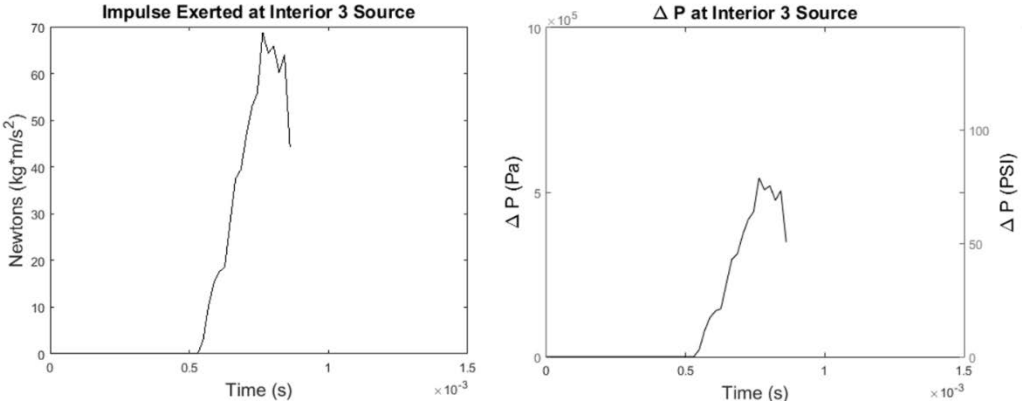

Fig. 9 Impulse and pressure measurements extracted from a blast gauge positioned at the I-3 source location resulting from detonation of 545 g of Detasheet C at the center of the MEFCT support structure

These results are consistent with predictions of the internal stresses and deformations as predicted using Velodyne continuum mechanics code. To simulate the deformations, the internal support structure was modeled without cassette and source elements. Instead, the 2 main support linkages were modeled with connectors of appropriate size at the source locations. Also, the charge was represented by a spherical charge of 545 g EL-506C (Detasheet C representative). Although some differences were apparent, the data compared well with that measured on the linkage structure, as the loading on this area is similar to that subjected by the simulation. The simulated displacements are shown in Fig. 10. In both the experimental and simulation, the rise of the dynamic deformations occurred over approximately 500 µs to a displacement magnitude of approximately 0.3 to 0.5 mm. The simulation rise began approximately 700 µs after detonation whereas the experimental results began near 500 µs after detonation. The results are similar enough to suggest this simplistic modeling method may be beneficial during the design phase of science experiments that will employ the MEFCT diagnostic, to ensure large overpressures will not be generated that could potentially harm the diagnostic.

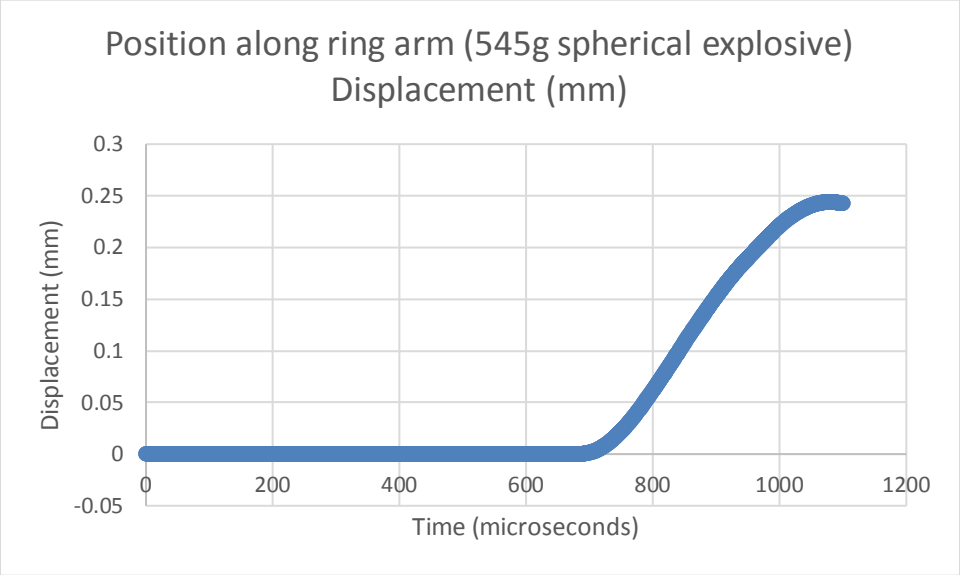

Fig. 10 Simulated displacement of the support linkage as calculated using a simplistic geometry in Velodyne continuum mechanics code

Although all components of the MEFCT diagnostic should endure the blast loading (although possibly not fragment impact), the importance of making in situ ring-displacement measurements to track the positions of the X-ray sources and detectors becomes evident from the magnitudes of elastic movements (indicated in Fig. 7). All of the sources within the MEFCT diagnostic were designed to generate X-rays from a 3-mm-diameter spot on the anode; and, all of the sources and

detectors are located approximately equidistant from the image to create similar image magnifications. Further, the orientations of the detectors were designed to be oriented normal to the source vectors. For experiments completing prior to the shock interaction with the support structure, no compensation for the source/detector positions will be necessary. However, if the X-ray flash occurs after the sources or detectors have moved, significant error could accumulate in magnification, parallax, or penumbra of the individual images. From the movements as measured in the 545-g high-explosive blast, one could expect the minimum error to include image magnification of 0.7% for an individual set of images, which could induce reduced contrast, image ghosting, and failure of regression analysis during the tomogram reconstruction.

It is also noted that a change in the position of the multiple pairs of sources and detectors will change the overall field of X-rays generated by the MEFCT diagnostic, as the flash X-ray sources produce X-rays through a large angular dependence. This is important because one cannot completely shield each detector to detect X-rays originating only from its intended source. Figure 11 depicts the angular dependence of X-ray dose from 150-, 300-, and 450-kV sources measured at 1 m[7] and a 2-D projection of how the X-rays from a 150-kV source fall off with a $1/r^2$ dependence in space. Figure 12 depicts a 3-D mapping of the numerous sources in a typical MEFCT configuration. This image shows that unintended X-rays will be detected by all detector plates. Because it is necessary to compensate for this phenomena by dividing all final images with a precollected source image, movement of the sources and detectors will be negatively affected. This can partially be compensated for using source projection software such as HADES, but this can only be accomplished if the real-time movement of the source–detector pairs is known.

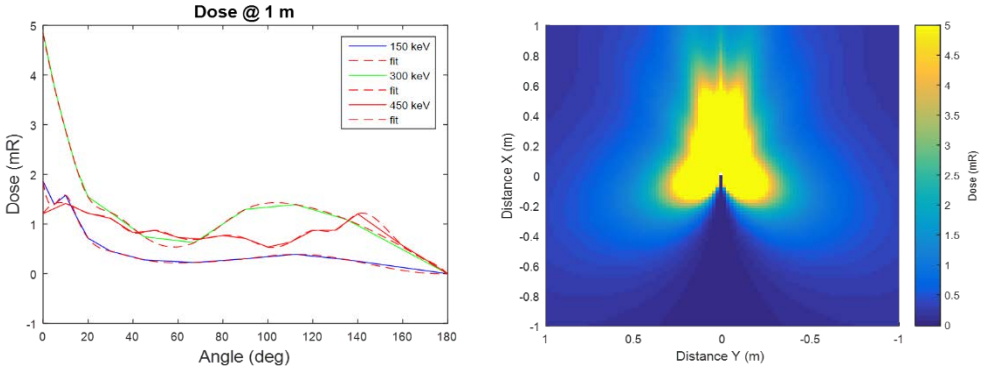

Fig. 11 Measurements of the radiation dose throughout the angular span of the 150-, 300-, and 450-kV flash X-ray sources used in the MEFCT diagnostic: left image shows the dose measured at 1 m throughout all angles, and right image shows a slice perpendicular to the source (located at [0,0]) depicting the radiation field and its $1/r^2$ characteristic decrease in intensity

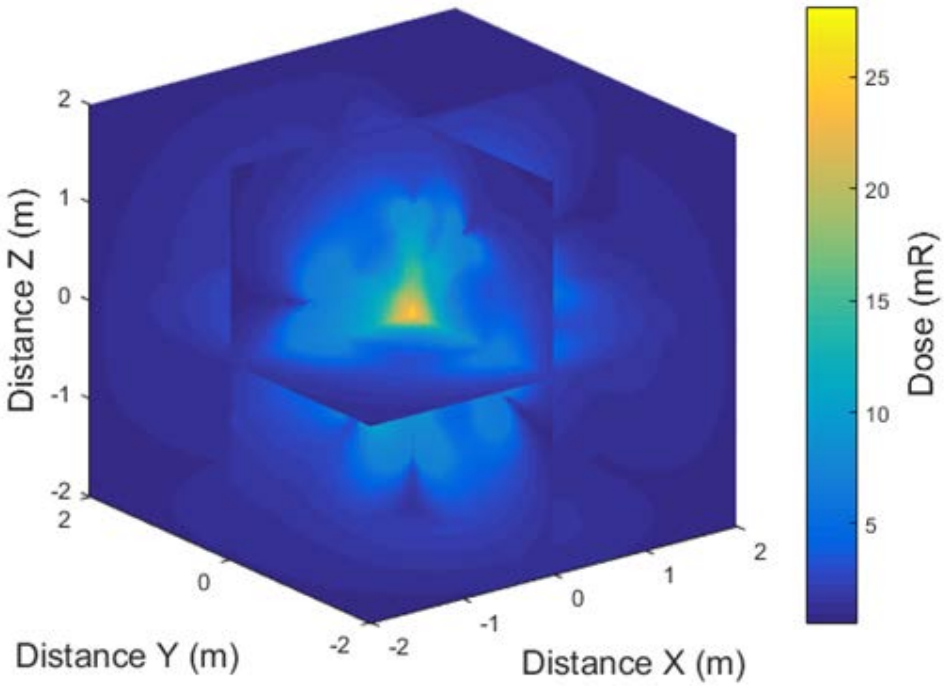

Fig. 12 Projected radiation dose depicting the asymmetries in intensity when numerous sources are combined within the MEFCT diagnostic

To incorporate movement of the sources into tomographic reconstruction codes, such as the Livermore Tomography Tools software platform or Ernst Mach Institute's High Speed Computed Tomography platform that uses the institute's Algebraic Recombination Technique, ARL has developed a code that inputs the initial positions of all source–detector pairs and the acceleration data acquired via PDV or accelerometers to give the positions at the time of X-ray generation.[21]

4. Conclusions and Implications

The interior ring of the MEFCT support structure has been tested for structural robustness. The ring was dynamically loaded by detonating up to 545 g of Detasheet C at its center. The dynamic motion of the ring was quantified using PDV, photography, accelerometers, and PDV blast gauges. It was determined that for loadings up to that generated by 364 g of Detasheet C at its center, the X-ray detector's shear tabs would not undergo complete failure. At loading of 545 g of Detasheet C, the tabs underwent complete failure and resulted in ejection as desired. For these loading scenarios, no plastic deformation was observed in the aluminum support structure or in the 3/4-inch (19-mm)-thick Grade 5 bolts that were used to affix the structure.

Measurements of the dynamic movement indicated that after approximately 0.5 ms, the ring would begin to deform elastically or via slip at the bolted joints. Peak deformations surpassed 8 mm within the first 4 ms after high-explosive detonation. This magnitude of movement is sufficient to cause significant distortion and error when attempting to compute the tomogram if not corrected for. It was also determined that, if necessary due to the timing of the desired X-ray flashes, PDV provided sufficient resolution of in situ measurements to track the location of the sources and detectors.

When used in a relatively simplistic, representative geometry, Velodyne worked well to predict the deflection of the ring. Similar simulations would be useful as a tool to predict the necessity of adding additional diagnostics, such as PDV, to make dynamic motion measurements of the source and detector elements of the MEFCT.

5. References

1. Schlomka JP, Roessl E, Dorscheid R, Dill S, Martens G, Istel T, Baumer C, Herrmann C, Steadman R, Zeitler G, Livne A, Proksa R. Experimental feasibility of multi-energy photon-counting k-edge imaging in pre-clinical computed tomography. Phys Med Biol. 2008;53:4031–4047.

2. Moser S, Nau S, Manfred S, Klaus T. In situ flash x-ray high-speed computed tomography for the quantitative analysis of highly dynamic processes. Meas Sci Technol. 2014;25:1–11.

3. Mishra D, Muralidhar K, Munshi P. A robust MART algorithm for tomographic applications. Num Heat Trans, part B: Fund Int J Comp Meth. 1999;35(4):485–506.

4. Mishra D, Longtin JP, Singh RP, Prasad V. Performance evaluation of iterative tomography algorithms for incomplete projection data. Appl Opt. 2004;43(7):1522–1532.

5. CUDA GPUs. Nvidia Accelerated Computing; [accessed 2016 July 21]. https://developer.nvidia.com/cuda-gpus.

6. Nvidia. Nvidia launches the world's first graphics processing unit: GeForce 256. 1999 Aug 31 [accessed 2016 July 21]. http://www.nvidia.com/object/IO_20020111_5424.html.5

7. L3 Applied Technologies. Flash x-ray seminar. San Leandro (CA); [accessed 2016 July 21]. http://www2.l-3com.com.

8. Carestream Dental LLC. Atlanta (GA); [accessed 2016 July 21]. http://www.carestreamdental.com

9. Champley K. Livermore tomography tools (LTT) technical manual. Livermore (CA): Lawrence Livermore National Laboratory; 2016 Mar 31. Manual No.: LLNL-SM-687016.

10. Cooper PW. Explosives engineering. New York (NY): Wiley-VCH; 1996.

11. Teledyne RISI. Tracy (CA); [accessed 2016 July 21]. http://www.teledynerisi.com.

12. Strand OT, Goosman DR, Martinez C, Whitworth TL, Kuhlow WW. Compact system for high-speed velocimetry using heterodyne techniques. Rev Sci Instr. 2006;77:083108-1–8.

13. Ao T, Dolan DH. SIRHEN: a data reduction program for photonic Doppler velocimetry measurements. Albuquerque (NM) and Livermore (CA): Sandia National Laboratories; 2010 June. Sandia Report No.: SAND2010-3628.

14. Doppler CJ. Über das farbige Licht der Doppelsterne und einiger anderer Gestirne des Himmels. Abhandlungen der Koniglich Bohmischen Gesselschaft der Wissenschaften. 1842;1:465–482.

15. Zellner MB, Randow CL, Cantrell R, Yonce CE, Strickland R, Perrella JA, Sturgill JM. Design of a simple blast pressure gauge based on a heterodyne velocimetry measuring technique. Aberdeen Proving Ground (MD): Army Research Laboratory (US). Report. Forthcoming 2016.

16. TME Third Millennium Engineering. Plano (TX); [accessed 2016 July 21]. http://tmeplano.com.

17. IPG Photonics. Oxford (MA); [accessed 2016 July 21]. http://www.ipgphotonics.com.

18. Keysight Technologies. Boeblingen, Germany; [accessed 2016 July 21]. http://www.keysight.com/main/home.jspx?cc=US&lc=eng.

19. AC Photonics. Santa Clara (CA); [accessed 2016 July 21]. http://www.acphotonics.com.

20. Peng W, Zhang Z, Gogos G, Gazonas G. Fluid structure interactions for blast wave mitigation. J Appl Mech. 2011;78:031016-1–7.

21. Uhlig K. Back-calculation of X-ray source and detector position. Aberdeen Proving Ground (MD): Army Research Laboratory (US). Report. Forthcoming 2016.

List of Symbols, Abbreviations, and Acronyms

2-D	2-dimensional
3-D	3-dimensional
CCD	charge-coupled device
I	Interior
MEFCT	Multi-Energy Flash Computed Tomography
PDV	photon Doppler velocimetry
TNT	2,4,6-trinitrotoluene

1 (PDF)	DEFENSE TECHNICAL INFORMATION CTR DTIC OCA
2 (PDF)	DIRECTOR US ARMY RESEARCH LAB RDRL CIO L IMAL HRA MAIL & RECORDS MGMT
1 (PDF)	GOVT PRINTG OFC A MALHOTRA
14 (PDF)	DIR USARL RDRL WMP A W UHLIG RDRL WMP C R BECKER B LEAVY RDRL WMP D J RUNYEON D PETTY M ZELLNER G VUNNI R DONEY K STOFFEL R CANTRELL C YONCE RDRL WMP E P SWOBODA D SCHALL D HACKBARTH